CROATICA CHEMICA ACTA CCACAA **61** (3) 685—717 (1988)

YU ISSN 0011-1643
CCA-1819 UDC 543.42
Author's Review

Orientational Order-Disorder Effects in Molecular Crystals as Evidenced by Low-Frequency Raman Spectra

G. N. Zhizhin, Yu. N. Krasjukov, E. I. Mukhtarov, V. N. Rogovoi, and N. V. Sidorov

Institute of Spectroscopy, USSR Academy of Sciences, Troitsk, Moscow region, 142092, USSR

Received 7 April, 1988

The studies of reorientational motions of molecules in crystals of organic compounds by low-frequency Raman spectroscopy are briefly reported. Some examples illustrate the efficiency of the investigation of order-disorder phenomena in organic crystals by the temperature dependence of low-frequency vibrational spectra combined with simultaneous calculations of the molecular dynamics by the atom-atom potentials (AAP) method. The conditions have been determined which are necessary in order to affect the low-frequency Raman spectra by anisotropy of molecular reorientations in crystals.

The study of disordered condensed matter properties is one of the actual problems in solid state physics. In recent years interest in the »order-disorder« phenomena and in the properties of disordered condensed phases of organic materials are risen. Organic crystals are extremely rich in disordered states because of the negligible intermolecular interaction. Polymorphic modifications, statistically and conformationally disordered states, liquid and plastic crystals — this is for sure an incomplete list of different forms of existence of the organic solid agregate state. This circumstance makes them convenient model objects for studying the physics of »order-disorder« processes.

The structure disordering processes which occur in a crystal as it approaches the melting point are to a great extent a display of the single complicated process of crystal melting. Pople and Karasz's statistical model[1] is one of the first theories of molecular crystal melting. The molecules in the lattice may be either in sites or between them and may have only two allowed orientations. It is also supposed that at $T = 0$ K the crystal is ideally ordered.

The main parameters of the model are the positional Q and orientational S order parameters and the molecular orientational diffusion barrier ν.

For small ν the model describes a phase transition into a plastic state. The orientational disorder in this case occurs at a temperature below the melting point. For large ν, a transition into the liquid crystalline state occurs. At intermediate ν values, orientational and positional »melting« takes place

simultaneously. Transformation to the plastic phase, depending on ν value, can be a first-or a second-order phase transition. In both cases the orientational disorder grows continuously with the temperature increase.

Amzel and Becka[2] extended the Pople and Karasz model by introducing an arbitrary number of orientations determined from symmetry considerations of the molecules and the crystal. This model allowed correct calculation of the configurational contribution to the entropy of the transition into the plastic phase. A detailed analysis of the lattice models of molecular crystals melting can be found in[3-6]. One of the important consequences of these models is the strong influence of the molecular geometry on the behaviour of molecular crystals in the course of melting, as is evidenced by the existence of intermediate disordered phases in the temperature range between the anisotropic crystal and the isotropic liquid. The models describe quailtatively the phase diagram for small ν values. However, assuming that the reorientational motion is substantially isotropic, these models do not embrace all the diversity of phenomena and give, generally speaking, a too simplified pattern of disordering during the phase transition. As shown in[7], the inclusion of reorientations of molecules with two different barriers ν_1 and ν_2 ($\nu_1 < \nu_2$) and the number of allowed orientations D_1 and D_2, respectively, causes — depending on the relationship between the model parameters — one or two phase transitions, induced by the orientational melting, and a phase transition with positional disordering of molecules. For sufficiently large D_2 depending on ν_2, three cases may be realized: activation of anisotropic reorientations of molecules just at the ordered phase and subsequent melting: activation of reorientations only with small barriers ν_1 to form a one-dimensional plastic crystal (reorientations with the barrier ν_2 are »frozen« up to the positional melting temperature); sequential reorientational activation of molecules with different barriers to form two plastic phases with different degrees of disorder.

The stepwise »melting« of the rotational degree of freedom can be seen by low-frequency Raman spectra. The Raman lines corresponding to librational vibrations are usually the most intensive and are, as a rule, related to molecular rotational vibrations with respect to their axes of inertia.

Usually the reorientational process of molecules is described by a correlation time τ_c characterizing the averaged life-time of the molecule in the state of small vibrations[8,9]. The number of molecules with the energy sufficient for overcoming the potential barrier V_{or} is proportional to $\exp(-V_{or}/kT)$ so for τ_c the temperature dependence is as follows:

$$\tau_c = \tau_o \exp(-V_{or}/kT) \tag{1}$$

The spectral intensity distribution of the scattered light in a general case is defined by the Fourier transform of the time autocorrelation function[10]:

$$C_{\varrho\sigma}(\tau) = \langle \alpha^*_{\varrho\sigma}(0)\, \alpha_{\varrho\sigma}(\tau) \exp(-i\omega_o\tau) \rangle \tag{2}$$

where $\alpha_{\varrho\sigma}$ is the polarizability tensor element of the crystal, ω_o is the frequency of the incident radiation. Considering the interruption of molecular vibrations by its random reorientations as a relaxation process, $C_{\varrho\sigma}(\tau)$ can be written as follows[10]:

$$C_{\varrho\sigma}(\tau) \sim \exp[i(\omega_j + \omega_o)\tau] \exp(-\tau/\tau_c). \tag{3}$$

It results in a Raman line of the Lorentzian shape and of the width

$$\Delta\omega_j = \frac{2\pi}{\tau_c} = \frac{2\pi}{\tau_o} \exp(-V_{or}/kT) \tag{4}$$

Thus, the qualitative analysis shows that the broadening of Raman lines by molecular reorientations depends exponentially both on the orientational barrier and the temperature.

Thus, either a structureless wing of the Rayleigh line or some very broad bands have been observed in the Raman spectra of plastic phases with small values of V_{or} and existing at the elevated temperatures. One would also expect that as the temperature increases, the anisotropic phase Raman lines related to the molecular vibrations around the axis in respect to which the orientational motion is activated will broaden and decrease in their intensity faster than the other[11]. Therefore, it is necessary for the molecules to be optically anisotropic relative to the reorientational axis and for the random molecular jumps to modulate directly the scattered radiation. Actually, if the molecular polarizability tensor in a crystal is

$$\hat{\alpha}_o = \begin{pmatrix} \alpha_{\parallel} & 0 & 0 \\ 0 & \alpha_{\perp} & 0 \\ 0 & 0 & \alpha_{\perp} \end{pmatrix} \tag{5}$$

where $\alpha_{\parallel}$ and $\alpha_{\perp}$ are the polarizabilities along the molecular reorientational axis and perpendicular to it, then in the stationary coordinate system the polarizability tensor will not depend on the rotational angle of the molecule around this axis:

$$\hat{\alpha} = \hat{A}^{\top}(\varphi_{\parallel}, \psi_{\perp}, \zeta_{\perp})\, \hat{\alpha}_0\, \hat{A}(\varphi_{\parallel}, \psi_{\perp}, \zeta_{\perp}) = \alpha(\psi_{\perp}, \zeta_{\perp}) \tag{6}$$

where $A(\varphi_{\parallel}, \psi_{\perp}, \zeta_{\perp})$ is the Euler matrix. Accordingly, the correlation function (2) will be determined only by the time dependence of the molecular rotational angles around the axes perpendicular to the reorientational axis.

In Figure 1 the Raman spectra of lattice vibrations for 1,12-dicarboclosododecarborane (para-carborane) are shown[12]. This compound has two plastic modifications (crystals I and II) with the phase transition temperatures 240 K and 303 K, respectively. The low-temperature modification spectrum with the narrow and strong lines is typical for the spectra of »rigid« crystals; in crystal I the structureless Rayleigh wing is typical of the spectrum of a plastic phase with completely disordered rotational orientations; the presence of the »crystalline« frequencies (50 and 70 cm^{-1}) in the spectrum of the low-temperature plastic modification II is indicative of the reorientational motion anisotropy of para-carborane molecules in this phase.

The small anisotropy of such reorientations is also retained in the low-temperature plastic modification of cyclopentane as we have established from the absorption spectra in the far IR region (Figure 2). Crystal I exists in the temperature range 176.8—138.1 K, crystal II — in the range 138.1—122.4 K; below 122.4 K an anisotropic crystal III is formed. Raman spectra of the cyclopentane II and cyclopentane I are typical for the plastic crystals spectra, and look as a broad structureless wing of the Rayleigh scattering line, and are not shown in Figure 2a. In the far IR spectrum of the crystal II (see Figure 2b,

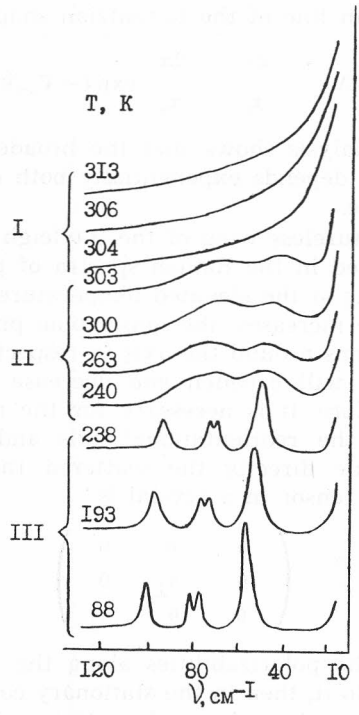

Figure 1. Low-frequency Raman spectrum temperature dependence for polycrystalline *n*-carborane[12].

126 K) two smeared absorption maxima can be observed in the regions near 60 and 85 cm^{-1} against the background of a very broad diffuse band. These maxima are absent in the spectra of the crystal I and of the liquid[13].

Another example can be a thiophene crystal undergoing several orientational phase transitions at the temperatures 112 K (IV—III), 138 K (III—II), 171 K (II—I)[8,14,15]. In Figures 3 and 4 the Raman spectra temperature dependence of the polycrystalline thiophene is shown measured in the range 77—260 K[16]. It is evident from Figure 3 that the spectrum of the phase IV is essentially different from the spectra of the other thiophene phases. The lines of this spectrum are the most pronounced and this fact indicates that the structure of the crystal IV is better ordered than the other phases. The most intensive line 54 cm^{-1} in the thiophene IV Raman spectrum broadens faster than the others as the crystal approaches its phase transition point IV—III (Figure 4), its intensity decreases and finally it disappears totally from the spectrum in the narrow temperature range of 1 K without changing of frequency. It may be assumed that this anomalous temperature dependence is related with the appreciable molecular orientational mobility observed in the NMR spectra of the phase IV[8]. In this case the band 54 cm^{-1} can be assigned to the thiophene molecular librations around the axis perpendicular to the molecular plane presenting the most probable reorientations. Thus, the phase transition IV—III is accompanied by the beginning of the thiophene mole-

cular reorientations in its plane and leads to the formation of a one-dimensional plastic crystal. Subsequent transitions are, apparently, accompanied only by further increase of the anisotropic orientational mobility of the molecules. It is confirmed by small values of transition entropies[8] and slight changes in Raman (Figure 3) and far IR absorption spectra[15,17].

Our conclusions about the increase of the molecular orientational mobility at phase transitions III—II—I in thiophene were confirmed in[18], where it was shown by X-ray studies that in thiophene I the orientational jumps around the axis perpendicular to the molecular plane are possible between twenty equivalent orientations, while in thiophene II they are possible only between ten such orientations.

It is interesting to compare the results for thiophene with the investigations of the furane crystal whose molecule is very similar to that of thiophene. Unlike thiophene furane has only two crystalline phases. Furane II is ordered $P4_12_12$ or $P4_32_12$, $Z = 4$[19]. Thiophene I and furane I have the similar disordered crystal lattices (Cmca or $Aba2$, $Z = 4$)[19,20]. It was determined by NMR data[21], by dielectric measurements[22] and X-ray studies that in furane I the molecules make orientational jumps around the axis perpendicular to the molecular plane and these jumps are possible between four equivalent orientations. The Raman spectrum of furane I external vibrations[24] (Figure 5),

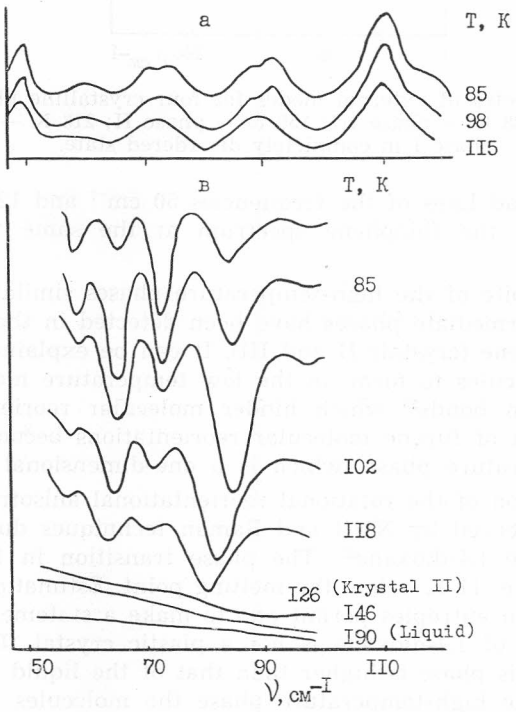

Figure 2. Raman (a) and far infrared absorption (b) spectra of cyclopenthane at different temperatures.

I, II — plastic modifications; III — ordered phase.

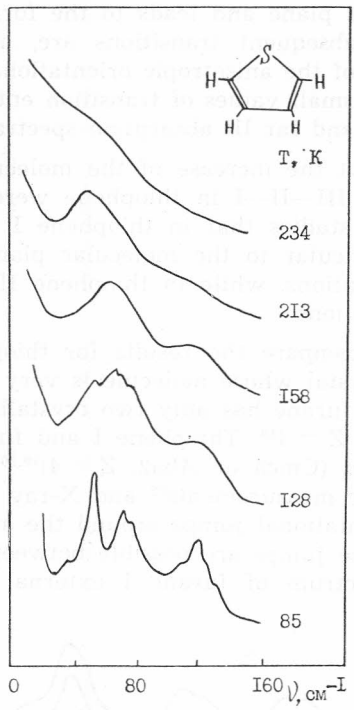

Figure 3. Raman spectra of external modes for four crystalline phases of thiophene 85 K — phase IV; 128 K — phase III; 158 K — phase II; 213 K — phase I; 234 K — phase I in completely disordered state.

containing two broad lines of the frequencies 50 cm^{-1} and 120 cm^{-1} at 158 K, is very similar to the thiophene spectrum at the same temperature (see Figure 3).

However, in spite of the high-temperature phases similarity of thiophene and furane no intermediate phases have been detected in the later which are observed in thiophene (crystals II and III). It can be explained by the ability of the furane molecules to form, in the low temperature modification, intermolecular hydrogen bonds[25] which hinder molecular reorientations. An appreciable activation of furane molecular reorientations becomes possible only in the high temperature phase, which is a one-dimensional plastic crystal[26].

The phenomenon of the rotational reorientational anisotropy of the molecules was also observed by NMR and Raman techniques during phase transition in crystalline 1,4-dioxane[27]. The phase transition in 1,4-dioxane takes place at 272.9 K, *i. e.* 11 K below the melting point. Estimation of the melting and phase transition entropies permit one to make a statement that the high-temperature phase of 1,4-dioxane is not a plastic crystal. The fact that the heat capacity of this phase is higher than that of the liquid justifies the supposition that in the high-temperature phase the molecules have appreciable rotational mobility. The analysis of the Raman spectra also confirms this conclusion. It is evident from the temperature dependence of the spectra (Figure 6) that the group of lines near 150 cm^{-1} observed at 85 K is smeared

out into the Rayleigh line wing during phase transition, whereas the rest of the lines in the phonon spectrum do not undergo any appreciable changes.

The conclusions about the molecular motion in the anisotropic phase and the changes in its structure during the phase transition in the above examples being drawn only on the basis of the temperature spectral evolution are inevitably speculative, because the interpretation of the vibrational transitions for these compounds is either totally lacking or has been carried out on the basis of indirect data and, consequently, is not absolutely right.

As a consequence, calculations of the dynamic and other properties of molecular crystals by means of the atom-atom potentials (AAP) describing intermolecular interaction, are important for a correct interpretation of spectral data and extraction of necessary information from them.

Beginning with the works of Kitaigorodskii[30] and Pawley[31] the AAP method is widely used for the calculation of frequencies and normal coordinates of external vibrations of molecular crystals. The interpretation of the molecular crystalline low-frequency spectra by means of the AAP method is exemplified in[32–35].

Normal vibrations are calculated in a general case by the method[36] solving a secular equation:

$$\left| F_{\mu l}^{\nu_m}(\vec{k}) - [\lambda(\vec{k}) - \lambda_b]\,\delta_{\mu\nu}\,\delta_{lm} \right| = 0 \qquad (7)$$

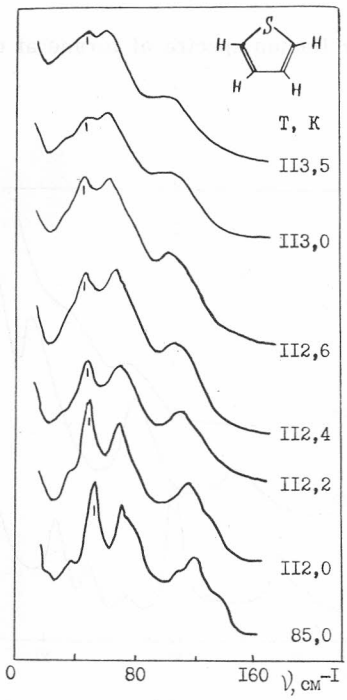

Figure 4. Temperature behaviour of the line 54 cm^{-1} in the external Raman spectrum of thiophene in the vicinity of the phase transition IV—III.

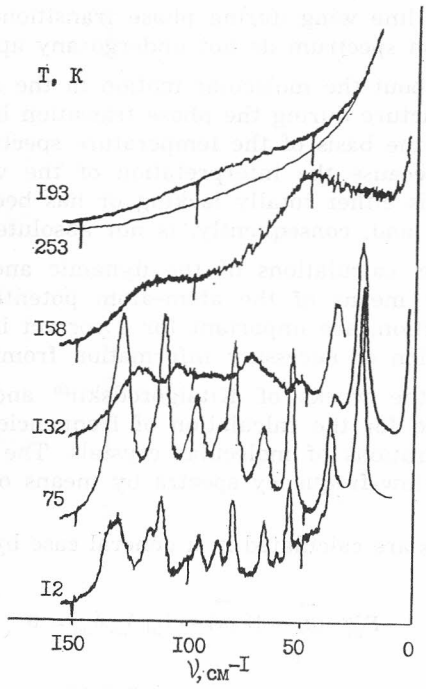

Figure 5. Low-frequency Raman spectra of furane at different temperatures[24].

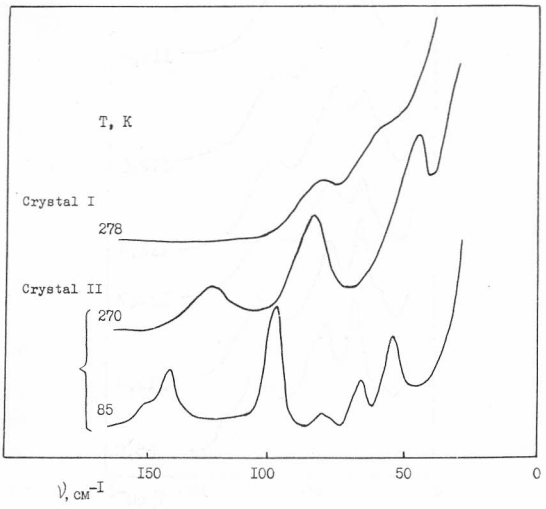

Figure 6. Temperatures at dependence of external Raman spectra of 1,4-dioxane crystal[27].

where $\lambda(\vec{k}) = 4\pi^2\nu^2(\vec{k})$, $\lambda_b = 4\pi^2\nu_b^2$, $\nu(\vec{k})$ and ν_b are the frequencies of normal vibrations for a crystal and a free molecule, respectively. $F_{\mu l}^{\nu m}(\vec{k})$ are the dynamic matrix elements.

Relative Raman line intensities are calculated by the oriented gas approximation according to the formula[37]:

$$I_{\varrho\sigma}(Q) = \frac{\text{const}}{\nu\,[1 - \exp(-h\nu/kT)]} \left| \frac{\partial \chi_{\varrho\sigma}}{\partial Q} \right|^2 \tag{8}$$

$$\overset{\wedge}{\chi} = \sum_m \overset{\wedge}{\pi}_m \alpha \overset{\wedge\wedge}{\pi}_m{}^T$$

where $\chi_{\varrho\sigma}$ is the ρ, σ-th element of the polarizability tensor of the crystalline unit cell, Q is the normal coordinate, $\overset{\wedge}{\pi}_m$ is the molecular cosine directed matrix, α is the polarizability tensor[38].

A characteristic feature of systems with the »order-disorder« phase transitions is the strong anharmonicity, which does not permit the description of the system behaviour near the transition in the harmonic or quasi-harmonic approximation. The only opportunity here is a direct calculation of the correlation function (2) by molecular dynamic methods using a sufficiently realistic intermolecular interaction model. This is a rather tedious and expensive problem[39].

This circumstance determines the main methodical approach to the study of organic crystals in the vinicity of phase transitions of the types »anisotropic crystal-plastic crystal« or »anisotropic crystal-isotropic liquid«. Recent investigations gave conclusive evidence that the knowledge of the normal coordinates of the external Raman spectrum of the low temperature anisotropic phase permits to follow experimentally the temperature evolution of the spectrum up to the phase transition and to connect it with the variation of the structure and of the other physical properties of the crystal.

This approach was used, in particular, in the study of the phase transition in 1,2-dichloroethane. The X-ray structure analysis[40], calorimetry[41] and NMR[42] data indicate that in this crystal, already in the low-temperature anisotropic modification, at increasing temperature the orientational jumps are activated presumably around the axis close to the line connecting Cl—Cl atoms. The phase transition occuring does not form an »isotropic«, but an one-dimensional plastic crystal.

This assumption is convincingly confirmed by the study of the low-frequency Raman spectra temperature dependence of 1,2-dichloroethane[43] (Figure 7). The intensity of the line 122 cm^{-1} (at 4.2 K) is assigned in [43] to librational vibrations around the axis close to that of Cl—Cl. With increasing temperature the intensity of this line decreases, it broadens faster than other lines and is absent in the high-temperature phase spectrum. The band 75 cm^{-1} (4.2 K) also assigned in [44] to the librations around the Cl—Cl axis behaves in the same way.

The phenomenon of rotational reorientation anisotropy was observed in a naphthalene crystal in the course of precise measurement of temperature dependence of low-frequency Raman spectra in the narrow premelting region[33,45].

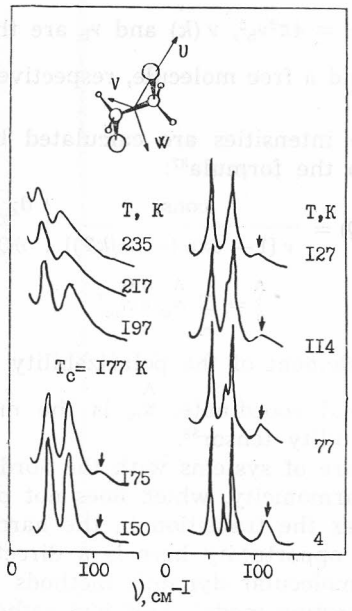

Figure 7. Raman spectra of external modes of dichloroethane-1,2 at different temperatures[43].

The naphthalene crystallizes at monoclinic syngony with a $P2_1/a$ space group and two molecules in the unit cell are in position C_i [29]. According to the group theory analysis in the Raman spectrum of this crystal six librational frequencies (3Ag + 3Bg) are active, while in the far IR spectrum three translational frequencies (2Au + Bu) are active. Low-frequency spectra of a naphthalene crystal were studied many times[46–50]. All the frequencies allowed by the selection rules have been detected. The experimental results and our calculations are summarized in Table I.

Calculations of the frequencies and normal coordinates[51] were made by means of AAP (6-exp) with Kitaigorodsky (AAP-1)[29] and Williams (AAP-2)[52] parameters, the summation radius 6 Å and with the use of the structure determined by an X-ray analysis at 300 K[53]. As seen from Table I the calculations are in good agreement with the experimental data for both sets of parameters.

Figure 8. shows the experimentally observed Raman spectra (Figure 8a) of naphthalene and also the calculated results for Raman line relative intensities in the oriented gas approximation (Figure 8b). The spectral lines are grouped in pairs of Ag and Bg species. As the temperature increases appropriate pairs merge into broad bands. The lines ν_5 A_g and ν_6 B_g which correspond to the librational molecular motion relative to the U′ axis, close to the axis U of the smallest moment of inertia, are much broader than the other and their bandwidths depend exponentially on temperature[50]. Attention is also drawn to the discrepancy between the temperature evolutions of the frequencies calculated in the quasi-harmonic approximation compared to the experimental one (Figure 9). This misfit is especially appreciable for ν_5 and

TABLE I

Frequencies and Shapes of External Modes of a Naphthalene Crystal

		a	*b*	*c**	
	w	0.840	0.320	—0.439	I_w = 564.4 a.m.u. Å²
A =	*v*	—0.442	0.871	0.372	I_v = 404.3 a.m.u. Å²
	u	—0.439	—0.213	0.873	I_u = 161.1 a.m.u. Å²

Symm.	$\nu_{exp.}$/cm⁻¹	$\nu_{calc.}$/cm⁻¹		Eigenvectors (AAP-2)					
	300 K	*AAP*-1	*AAP*-2	L_w	L_v	L_u	T_a	T_b	T_{c^*}
A_g	ν_5 109	115	110	0.108	0.569	0.815			
	ν_4 74	80	85	0.185	0.817	0.546			
	ν_2 50	54	56	0.979	0.092	0.192			
B_g	ν_6 125	94	106	0.039	0.080	0.996			
	ν_3 70	75	79	0.405	0.910	0.089			
	ν_1 46	41	47	0.914	0.407	0.003			
A_u	ν_7 98	93	93				0.812		0.584
	ν_8 53 [47]	55	50				0.584		0.812
B_u	ν_9 66	69	64					1.000	

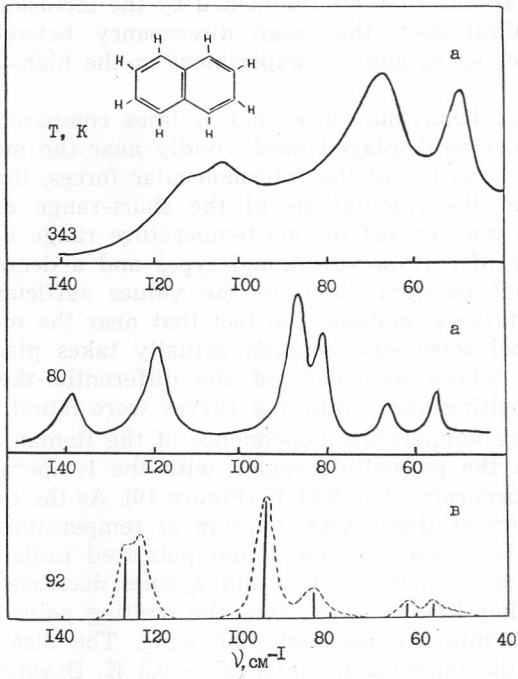

Figure 8. Experimental (a) and calculated (b) Raman spectra of external modes of a naphthalene crystal at different temperatures.

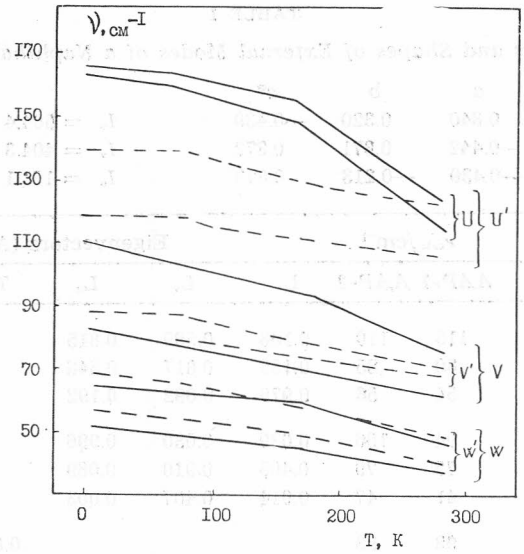

Figure 9. Temperature dependence of experimental and calculated (solid lines) frequencies in the external Raman spectrum of naphthalene.

ν_6 lines and this is, apparently, caused by strong anharmonicity of these vibrations[51]. If the general overrate of the calculated frequencies as compared to the experimental ones may be diminished by the inclusion of low-frequency intramolecular vibrations[54], the large discrepancy between the calculated frequencies of lines ν_5, ν_6, and the experiment in the high-temperature region holds true.

The anomalous behaviour of ν_5 and ν_6 lines compared to other phonon spectrum lines must be displayed most vividly near the melting point of the crystal. Due to attenuation of the intermolecular forces, the expansion of the crystal lattice and the fluctuations of the short-range order in molecular arrangements one may expect in this temperature range both an increase in the anharmonicity of certain vibrational types and a decrease of the appropriate orientational barriers down to the values sufficient to provide the molecular reorientational motion. The fact that near the melting point of the naphthalene crystal some subtransition actually takes place is indicated by the results of [55], where by means of the differential-thermal analysis the maxima on the melting and solidifying curves were found.

We studied the temperature dependence of the Raman spectra of a naphthalene crystal in the premelting region with the temperature step ~ 0.1 K and thermostatic accuracy of ± 0.01 K (Figure 10). As the lines in the external vibrations spectrum of this crystal overlap at temperatures above the room temperature, single crystal specimens and polarized radiation were used for the experiments One can see that ν_5 and ν_6 lines decrease in intensity much faster that the other Raman lines. Near the melting point the ν_5 and ν_6 lines are fully smeared into the Rayleigh line wing. The disappearance of these lines happens in the temperature interval ~ 0.3 K. Beyond 0.25 K up to the melting point these lines are practically unobservable, whereas the other lines of the external vibrational spectrum are clearly observed. As the tempera-

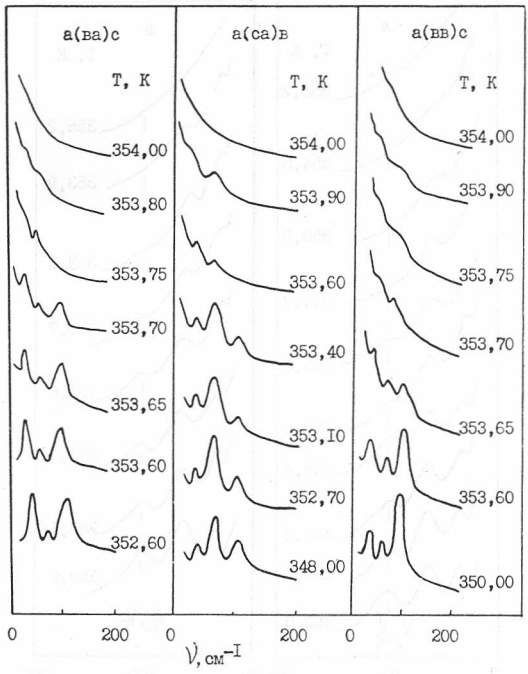

Figure 10. Temperature dependence of the external Raman spectra of naphthalene single crystal near the melting point.

ture decreases from 353.8 to 353.6 K the ν_5 and ν_6 lines appear in the spectrum again. The experiment was repeated with two single crystal specimens in four crystal orientations with excellent reproducibility.

The disappearance of ν_5 and ν_6 lines in the premelting region may be caused by their depolarization as the temperature of the single crystal approaches the melting point. Therefore, we carried out an additional study of polycrystalline naphthalene specimes (Fig. 11a). In the polycrystalline sample lines ν_5 and ν_6 in the premelting region are even more broadened and not resolved. Nevertheless, it is clearly seen that here also the lines smear in the Rayleigh line wing much faster than the other lines in the Raman phonon spectrum. This fact is also clearly demonstrated by Raman spectra of the naphthalene-β-naphthol mixture (Figure 11b). It is well known that, when an impurity is introduced, the temperature interval of the premelting effects in the crystal increases. We have chosen β-naphthol as an admixture because the crystalline structure of this mixture is well studied in wide ranges of temperatures and pressures[56,57]. For the selected concentration of the admixture (5%) the solid solution lattice is similar to the structure of a pure naphthalene crystal[57]. In spite of the fact that the increase in temperature interval of the effect in this case was not very much enlarged (apparently, not more than 0.5 K) (Fig. 11b), one can see distinctly from the spectra, as compared to the other spectral lines, the preferential disappearance of the lines which refer to the molecular librations around the U' axis.

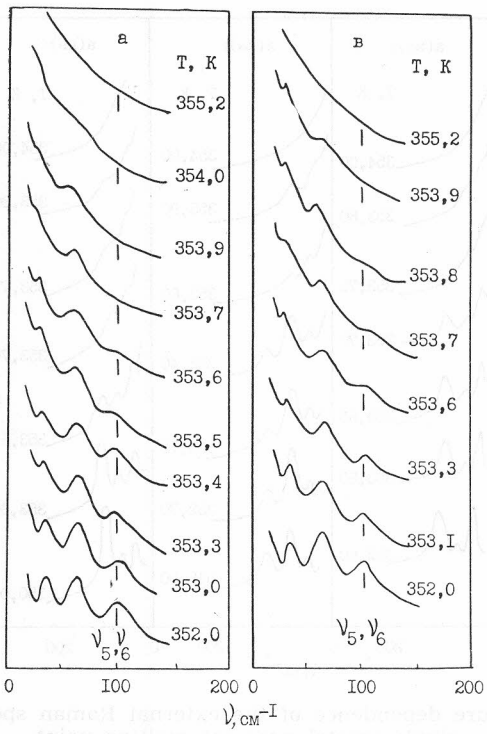

Figure 11. Temperature dependence of Raman spectra of external modes of naphtalene (Ma) and solid solution of naphthalene (95%) + β-naphthol (5%) (Mb) near the melting point.

Valuable information of the reconstruction character of the crystalline structure near phase transitions may be obtained from calculations of the reorientational molecular motion barriers. Calculations of the molecular reorientation barriers relative to their inertia axes in our case were made with the help of atom-atom potentials and AAP-2 parameters. Since there are no data on the crystalline structure for the temperatures near the melting point, the potential barriers were calculated only for the room temperature (Fig. 12). The rigid lattice approximation was used when the selected molecule rotates around its inertial axes, and the nearest environmental molecules are considered as motionless and positioned in accordance with the X-ray structural analysis data[29]. From the data obtained one can see that the smallest reorientational barrier appears when the molecule is rotating around the axis of the largest moment of inertia *W*. Two other barriers appearing during the rotations of the molecules around the *U* and *V* axes, are appreciably larger.

Attention is drawn to the barrier of reorientations around the axis *W*. The barrier is relatively large (~16 kcal/mol) and the curve has some sufficiently deep minima. It was shown by X-ray structural studies of the complex naphthalene-tetracyanbenzene that at 250 K in this crystal the naphthalene molecules have been randomly rotated in their plane inside an angle limit of 36°[58]. For this temperature the NMR signal begins to narrow

undicating the reorientational motion[57]. Calculation of the reorientation barrier around the axis perpendicular to the molecular plane made in[58] for a naphthalene-tetracyanobenzene complex gives a curve very close to ours for pure naphthalene (Figure 12). This permits one to suppose that for high temperatures in pure naphthalene a static disorder is realized (naphthalene molecules are statically disordered around the W axis inside an angle limit of $\sim 60^\circ$ with the preferential conservation of the orientations relative to other axes). The increase in the number of the irregularly oriented molecules results in the violation of the selection rules for the wave vector — the opening of the Brillouin zone and broadening of the lines. The preferential broadening of ν_5, ν_6 lines in this case may be explained by a strong dependence of the dispersion branches corresponding to these vibrations on the wave vector

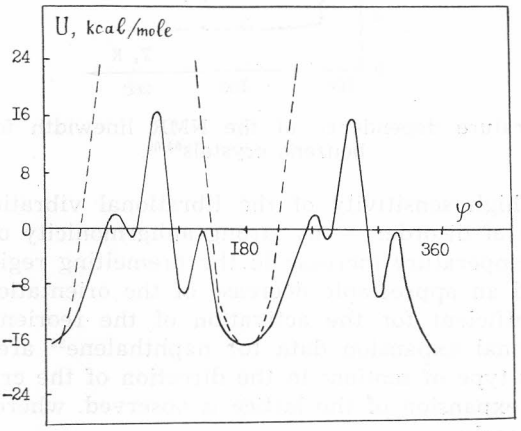

Figure 12. Dependence of the molecular potential energy in naphthalene on rotation angle φ around the W (solid curve) and V (dashed curve) axes at room temperature. During the molecular rotation around U axis the value of U_u is very large (216 kcal/mol) already at $\varphi = 40^\circ$ ($I_u < I_v < I_w$).

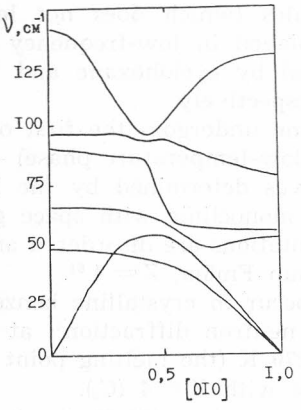

Figure 13. Dispersion curves in the direction [010] of the Brillouin zone for external modes of a naphthalene crystal. To the right: B_g and B_u modes, to the left: A_g and A_u modes[31].

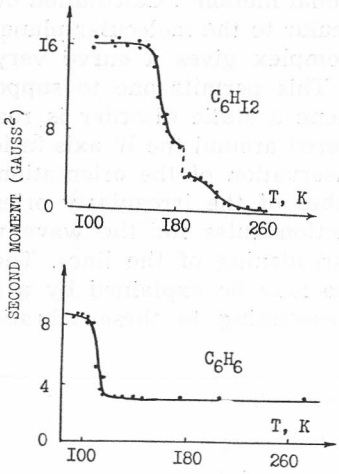

Figure 14. Temperature dependence of the NMR linewidth for cyclohexane and benzene crystals[64,66].

(Figure 13) and high sensitivity of the librational vibrations around the U axis to such type of disorder — by strong anharmonicity of these vibrations.

At further temperature increase in the premelting region one can expect redistribution and an appreciable decrease of the orientational barriers down to the values, sufficient for the activation of the reorientational molecular motion. The thermal expansion data for naphthalene[29] are indicative of the possibility of this type of motion: in the direction of the crystallographic axis a the anomalous expansion of the lattice is observed. whereas the parameters b and c vary linearly.

As it has already been noted, the optical anisotropy of the crystalline molecules relative to the reorientational axis is an indispensable condition for the rotational reorientation anisotropy in the Raman spectrum. In this respect it is interesting to ascertain how the wide spread reorientational motion of high-symmetric molecules (which does not lead to fluctuations in the crystal anisotropy) is displayed in low-frequency Raman spectra. Such molecules may be exemplified by cyclohexane and benzene with their propre symmetries D_{3d} and D_{6h} respectively.

At 186.1 K, cyclohexane undergoes the first order phase transition from anisotropic crystal II (the low-temperature phase) — to the plastic crystal I[60]. The crystal II structure was determined by the X-ray analysis at 115 K[61]. Cyclohexane crystal II is monoclinic with space group C2/c and $Z = 4$ (C_i). In crystal I molecular orientations are disordered and its structure is described by the effective space group Fm3m, $Z = 4$ [61].

No phase transitions occur in crystalline benzene at normal pressure. Its structure was defined by neutron diffraction[62] at 140 and 218 K as well as by X-ray diffraction[63] at 270 K (the melting point being 278 K). Space group of benzene crystal is Pbca with $Z = 4$ (C_i).

Beginning with the temperature 150 K, *i. e.* long before the phase transition to the plastic state of cyclohexane II, in the NMR spectrum an appreciable narrowing of the resonant line was observed (Figure 14) that was attributed

to the activation of reorientational motion of the molecules around their axis C_3 [64]. The values of the barrier obtained by the NMR temperature dependence measurements of the relaxation times T_1 and $T_{1\varrho}$ are 11 and 7 kcal/mol respectively[64,65]. It should be noted that the minima of these dependences almost coincide with the phase transition point at which the crystal structure and the character of the molecular motion change drastically. Therefore, such measurements can give only an approximate estimation of the barrier value.

In crystalline benzene a more drastic narrowing of the resonant NMR line takes place at 110 K[66] (Figure 14) *i. e.* long before the melting point. The values of the reorientational barrier of benzene molecules around their axis C_6 measured by the NMR method in papers[64,67,68] are equal to 3.7, 3.5 and 4.2 kcal/mol respectively. The calculated barriers which are close to the experimental values (2.7, 3.2 and 4.9 kcal/mol) were obtained in paper[29,68,69] using the AAP method and the crystalline structure measured at 140 K[62]. The barriers were determined by the change in the lattice energy during the rotation of the chosen molecules around the C_6 axis and with fixed positions of the neighbouring molecules (the rigid lattice approximation).

We performed an analogous calculation for the crystals of cyclohexane II and benzene as shown in Figure 15. The barrier values, obtained are 4.5 (cyclohexane II) and 3.2 kcal/mol (benzene). The hydrogen atoms repulsion which is very sensitive to changes in the distance between the molecules, and consequently to the thermal expansion of the crystal, contributes mostly to the barriers. In particular, the calculation for benzene has shown that the

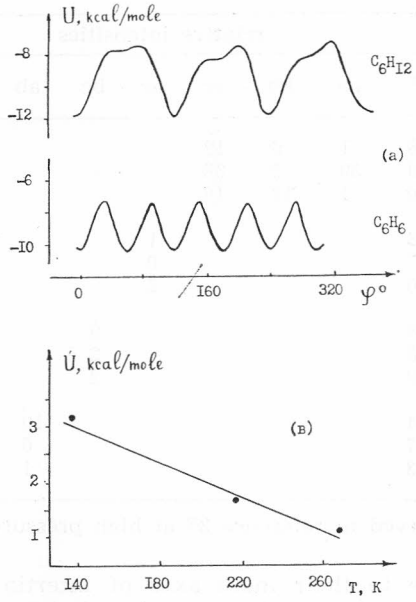

Figure 15. a. Dependence of the lattice energy of cyclohexane (115 K, AAP 4) and benzene (140 K, AAP 3) on the rotation angle of the molecule around the W axis. b. Calculated temperature dependence of the reorientation barrier for a benzene molecule around the W axis (AAP 3).

barrier value at 270 K is almost twice as low as that at 140 K (Figure 15b). In the case of cyclohexane the barrier sensitivity to the temperature must be still higher, since the number of H...H contacts in this crystal is considerably larger than in benzene. This fact must be used to explain the discrepancy between the calculation and the NMR data, which gives the barrier value averaged over some temperature range.

Thus, the calculated and experimental data indicate the existence of the molecular reorientational motion in the crystals of cyclohexane II and benzene around the molecular axes C_3 and C_6 respectively with the values of the orientational barriers very close. In order to study the display of these motions in low-frequency Raman spectra of polycrystalline benzene and cyclohexane II we performed measurements in a wide temperature region, including the closet vicinity of phase transitions.

In low- frequency Raman spectrum of benzene 12 external librational normal modes are active:

$$\Gamma(R) = 3A_g + 3B_{1g} + 3B_{2g} + 3B_{3g}.$$

Single crystal polarized Raman spectra were measured and calculated by the authors of[70] in the rigid molecule approximation using of AAP-1 (see Table II). The normal vibrations correspond mainly to molecular librations

TABLE II

Frequencies of Librational Vibrations and Relative Intensities of Raman Lines for a Benzene Crystal (140 K) Calculated by AAP-1 and at $\alpha_{uu} = \alpha_{vv} \neq \alpha_{ww}$ ($I_u = I_v < I_w$)

Symm.		exp.	calc.	relative intensities						assignment	
		(70), cm^{-1}	cm^{-1}	aa	bb	cc	ac	bc	ab	poly-cryst.	
A_g	ν_1	92	95.8	1	6	12				18.6	L_v, L_w, L_u
	ν_2	79	77.9	59	2	38				100.0	L_u, L_v
	ν_3	57	46.0	1	12	16				27.9	L_w
B_{1g}	ν_4	128	138.8				1			1.5	L_u
	ν_5	100	94.7				0			0.8	L_v
	ν_6	57	51.0				2			3.6	L_w
B_{2g}	ν_7	—	101.8					9		17.1	L_v
	ν_8	90	91.5					2		4.6	L_w
	ν_9	79	84.0					2		4.7	L_u
B_{3g}	ν_{10}	128	135.4						10	19.9	L_u
	ν_{11}	84*	86.7						0	0.4	L_w
	ν_{12}	61	65.3						1	2.4	L_v, L_w

* The line ν_{11} was observed in reference 35 at high pressures.

around the axes close to their main axes of intertia. In Table II and in Figure 16 are shown calculated relative Raman line intensities in the oriented gas approximation. It was supposed that the polarizability tensor of the molecule in the crystal has the form as presented in relation (5), *i. e.* the polarizability relative to the axes U and V in the molecular plane are equal.

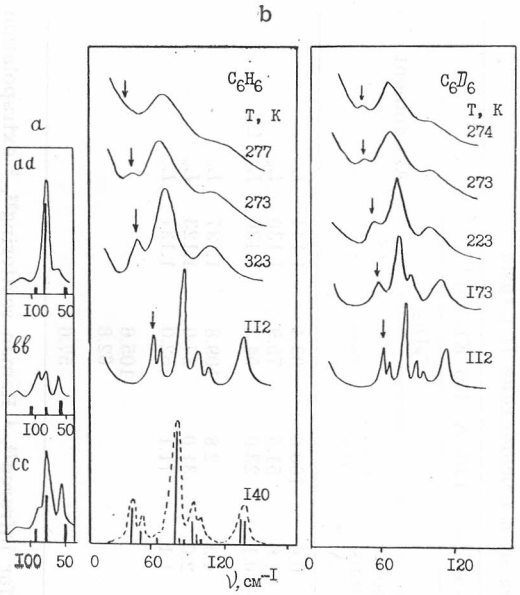

Figure 16. External Raman spectra of benzene measured at different temperatures and calculated spectrum (dashed lines) for $T = 140$ K.

This model simulates very well both mono- and polycrystal Raman spectra (Figure 16). Therefore, the rotational motion of benzene molecules around W axis (C_6 axis of a free molecule) gives a zero contribution to the Raman spectrum intensity. So, the appearance of random molecular reorientations around this axis is unlikely. In fact, the temperature changes in a benzene polycrystal Raman spectrum (Figure 16) point to a simultaneous broadening of all spectral lines. Under these conditions the line 57 cm^{-1} (140 K), which has a comparatively large intensity and refers to the normal vibration ν_3 with the predominant participation of molecular librations around the W axis (Table II) is observed in the spectrum up to the melting point (Figure 16).

In low-frequency Raman and far IR spectra of the low temperature phase II of cyclohexane six librational and three translational normal vibrations are active;

$$\Gamma(R) = 3A_g + 3B_g; \qquad \Gamma(IR) = 2A_u + B_u.$$

Low-frequency vibrational spectra of the cyclohexane crystal were studied by several authors[11,32,71-73]. The experimental data available for phase II are summarized in Table III. Since it is practically impossible to have a sufficiently large single crystal at low temperature because of the phase transition, the measurements were performed on the polycrystalline samples only. The assignment was performed on the basis of the lattice dynamics calculations and isotopic relationships.

The spectrum was calculated in the rigid molecules approximation, which is quite justified here, since the lowest intramolecular frequency of cyclohexane is 240 cm^{-1} hence twice as large as the highest frequencies of external vibrations. The AAP had not been used before to describe the properties of

TABLE III

Interpretation of Low-Frequency Vibrational Spectra of a Cyclohexane II Crystal

Symm.		Experiment, cm^{-1}					Calculation (AAP-4, d_{CH} = 1.07 Å, 115 K), cm^{-1}						Assignment
		C_6H_{12}		C_6D_{12}		$\frac{\nu_H}{\nu_D}$	C_6H_{12}				C_6D_{12}		
		1) 4.2 K	2) 77 K	3) 115 K	4) 115 K	115 K	$\nu_{harm.}$	Anharmonic corrections $\Delta\nu^{(3)}$	$\Delta\nu^{(4)}$	$I_{ntensity}$ (%)	$\nu_{harm.}$	$\frac{\nu_H}{\nu_D}$	
A_g	ν_1	120	115	110	97	1.13	102.3	—0.1	0.6	100.0	89.4	1.144	L_v
	ν_2	94	90	85	75	1.13	85.8	—1.5	1.6	51.5	75.9	1.130	L_u
	ν_3	77	74	69	61	1.13	61.0	—1.2	—0.1	23.0	54.3	1.130	L_w, L_u
B_g	ν_4	138	128	120[5]	—	—	124.8	—	4.3	2.8	109.8	1.137	L_u
	ν_5	102	99	92	83	1.11	97.7	—	2.0	31.0	87.0	1.123	L_w
	ν_6	66	64	62	54	1.15	59.1	—	1.1	71.1	52.0	1.137	L_v
A_u	ν_7	—	101	98	—	—	112.9				105.6		
	ν_8	—	—	—	—	—	67.2				62.8		
B_u	ν_9	—	—	61	—	—	61.6				57.6		

Notes: [1] Raman scattering[11], [2] Raman scattering[72], [3] Raman scattering[32], far infrared[73], [4] Raman scattering[32], [5] extrapolation for 115 K for frequencies 138 cm^{-1} (4.2 K) and 128 cm^{-1} (77 K)[72].

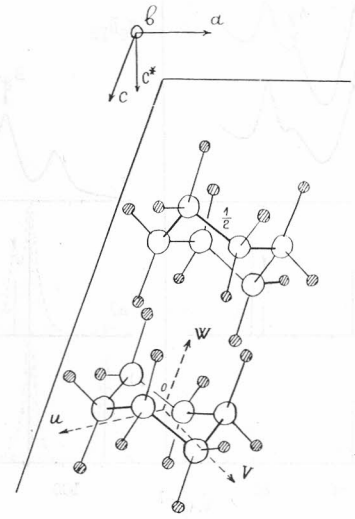

Figure 17. Fragment of a crystallographic cell of cyclohexane II. ○ — carbon atom, ● — hydrogen atom, *U*, *V*, *W* are inertial axes of the molecule.

a cyclohexane crystal and, therefore, different sets of parameters, noted as AAP-1—AAP-4, were tried in the calculation. A cyclohexane molecule has a large number of hydrogen atoms forming short H . . . H contacts in the crystal (Figure 17). Therefore, the inaccuracy in the determination of the coordinates for these atoms which is inherent to the X-ray method, can influence rather strongly the calculation results. Consequently, the lengths of all C—H bond lengths were supposed to be equal and were varied in the normal vibrational calculations within the limits of 1.00—1.10 Å. The influence of the calculation conditions on the frequencies of external vibrations is illustrated in Table IV. The best agreement with the experiment is observed for the set of parameters AAP-4 and the C—H bondlength $d_{CH} = 1.07$ Å.

TABLE IV

Frequencies of Normal Vibrations (cm^{-1}) of a Cyclohexane II Crystal (115 K) Calculated with Different Lengths of C—H Bonds (Å) and AAP Parameters

Symm.	d_{C-H} X-ray	AAP-4 1.03 Å	AAP-4 1.05 Å	AAP-4 1.07 Å	AAP-4 1.09 Å	AAP-3 1.07 Å	AAP-1 1.05 Å	AAP-2 1.05 Å
	87.5	93.6	97.9	102.3	106.8	100.1	114.4	111.0
A_g	78.0	78.6	82.1	85.8	89.7	83.9	95.8	92.8
	60.5	57.1	59.0	61.0	63.0	60.5	69.0	59.0
	102.0	113.2	118.9	124.8	131.0	123.0	140.3	145.3
B_g	82.0	88.7	93.1	97.7	102.5	96.5	110.3	111.8
	55.9	53.1	56.0	59.1	62.3	59.3	68.5	55.1
	94.6	104.0	108.4	112.9	117.5	109.5	124.4	118.5
A_u	57.5	62.1	64.6	67.2	69.9	66.3	74.9	75.5
B_u	57.6	54.9	58.1	61.1	65.3	61.3	70.3	69.9

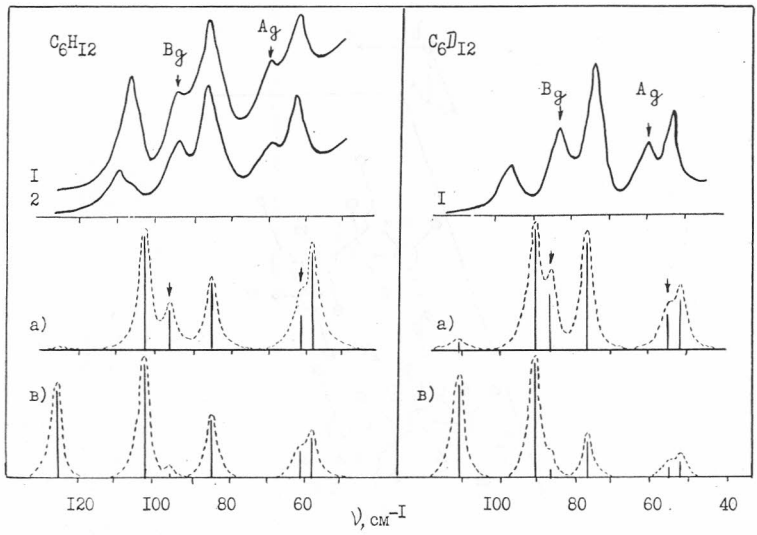

Figure 18. Observed (solid lines) and calculated (dashed lines) frequencies and intensities of the external Raman spectra of cyclohexane II crystal. The arrows indicate the bands ν_3 (Ag) and ν_5 (Bg) corresponding predominantly to the libration arround the axis W.

The interpretation of the low-frequency cyclohexane vibrational spectrum in Table III is based on the calculation in the quasi-harmonic approximation. Taking into account large mobility of the molecules in this crystal some anharmonic corrections for librational vibration frequencies are given in Table III. They were calculated applying the model of independent oscillators[74]. The corrections proved to be very small and did not affect the interpretation of the spectrum.

The cyclohexane molecule shape with the symmetry group D_{3d} is practically retained in the crystal (Figure 17). Therefore, in the calculation of relative Raman line intensities it was perfectly natural to suppose that, analogously to benzene, cyclohexane molecules in the crystal II are optically isotropic relative to their rotation around the W axis (C_3 axis of the free molecule, see Figure 17). However, the Raman spectrum calculated by this model does not agree with the experiment (Figure 18). In particular, the calculation predicts for 115 K a considerable intensity of the line ν_4 which is of the highest frequency. This band was not observed at all in the Raman spectrum at this temperature and appears only at much lower temperatures[11,72]. Thus, in contrast to benzene, the oriented gas approximation is unfit here.

For the calculation of the intensities we used the effective polarizability tensor of the molecule in the crystal[75]; this tensor empirically takes into account the influence of the local internal field and of the intermolecular interaction. The effective polarizability tensor used was:

$$\overset{\wedge}{\alpha} = \begin{pmatrix} \alpha_{uu} & \alpha_{uv} & 0 \\ \alpha_{uv} & \alpha_{vv} & 0 \\ 0 & 0 & \alpha_{ww} \end{pmatrix}, \quad \alpha_{uu} = \alpha_{vv} \neq \alpha_{ww}. \tag{9}$$

Since we discuss the relative line intensities, the derivatives of the tensor (9) with respect to the rotational angles of the molecule around its axes of inertia can be expressed in terms of a single varying parameter:

$$\frac{\partial \alpha}{\partial \varphi_u} = \begin{pmatrix} 0 & 0 & \alpha_{uv} \\ 0 & 0 & \alpha_{vv} - \alpha_{ww} \\ \alpha_{uv} & \alpha_{vv} - \alpha_{ww} & 0 \end{pmatrix} \rightarrow \begin{pmatrix} 0 & 0 & k \\ 0 & 0 & 1 \\ k & 1 & 0 \end{pmatrix}$$

$$\frac{\partial \alpha}{\varphi_v} = \begin{pmatrix} 0 & 0 & \alpha_{ww} - \alpha_{uu} \\ 0 & 0 & -\alpha_{uv} \\ \alpha_{ww} - \alpha_{uu} & -\alpha_{uv} & 0 \end{pmatrix} \rightarrow \begin{pmatrix} 0 & 0 & -1 \\ 0 & 0 & -k \\ -1 & -k & 0 \end{pmatrix} \qquad (10)$$

$$\frac{\partial \alpha}{\partial \varphi_w} = \begin{pmatrix} -2\alpha_{uv} & 0 & 0 \\ 0 & -2\alpha_{uv} & 0 \\ 0 & 0 & 0 \end{pmatrix} \rightarrow \begin{pmatrix} -2k & 0 & 0 \\ 0 & 2k & 0 \\ 0 & 0 & 0 \end{pmatrix}$$

k being the only varied parameter and

$$\alpha_{uv} = k\,(\alpha_{vv} - \alpha_{ww}) = k\,(\alpha_{uu} - \alpha_{ww}).$$

In Figure 18 and in Table III the results of calculations are presented for $k = 0.9$, which gives the best agreement with the experiment. Taking into account the sufficiently rough approximations of this model, the agreement with the experiment should be considered as satisfactory.

Thus, unlike benzene, a cyclohexane molecule in the crystal II becomes optically anisotropic with respect to its axis C_3. Consequently, one may expect in the Raman spectrum a direct display of the reorientational molecular motion around this axis. In Figure 19 the temperature dependence of

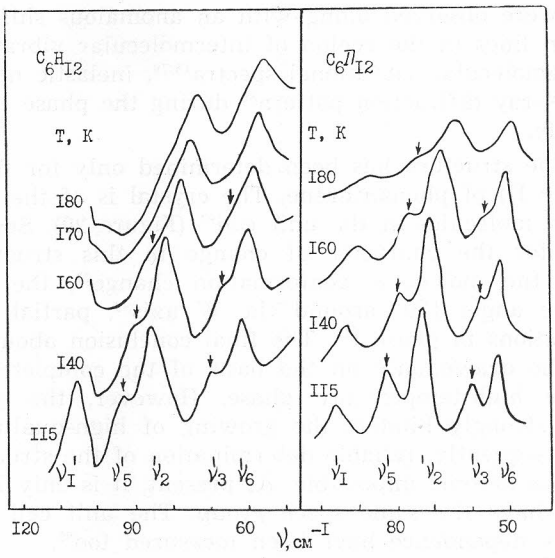

Figure 19. Temperature dependence of low-frequency Raman spectra of cyclohexane and deuterocyclohexane. Arrows indicate the librational modes arround W axis.

low-frequency Raman spectra of cyclohexane and deuterocyclohexane polycrystals in the region 115—180 K is shown. First of all one can see that ν_3 and ν_5 lines are broadening and their intensities decrease faster than of the others as the phase transition is approached. At 160—170 K, *i. e.* 20—30 degrees before the transition point, they become practically unobservable. From the normal coordinates calculation (Table III) it follows that $\nu_3 (A_g)$, $\nu_5 (B_g)$ lines refer to the vibrations with the preferential participation of molecular librations around the axis *W* (Figure 17). The other Raman spectral lines corresponding to the librations of molecules around other axes *U* and *V* are clearly observed up to the temperatures which differ from the transition point by no more than 0.2 K[11,32]. From these experiments it follows that molecular reorientations around *U* and *V* axes in the anisotropic phase are essentially hindered and are »released« only during the transition into the plastic crystal, whereas reorientations around *W* axis are activated in the crystal II long before the transition occurs.

Thus, having the normal coordinates of external modes active in the Raman spectrum and studying the temperature dependence of this spectrum, one can obtain valuable information on the anisotropy of the molecular reorientations in the crystal. Hence, it is necessary for the molecule in the crystal to be optically anisotropic, relative to the axis around which the reorientational motion is activated.

In connection with the phenomena considered in this paper the studies of the phase transition in phenanthrene by low-frequency Raman spectra are of independent interest. The crystalline phenanthrene ($C_{14}H_{10}$) has already for a long time been an object of active research by different physical methods. This interest is due to the presence of an unusually smeared high order phase transition in the temperature interval 315—345 K. Appreciable anomalous changes in the electric conductivity[76], dielectric constant[77], thermal expansion of the crystal[78] were observed along with an anomalous shift of Raman and far IR absorption lines in the region of intermolecular vibrations[15,79]. On the other hand, intramolecular vibrational spectra[15,79], inelastic neutron scattering spectrum[77] and X-ray diffraction pattern[80] during the phase transition change only very slightly.

The crystalline structure has been determined only for the low-temperature phase (phase II) of phenanthrene. The crystal is of the space group $P2_1$ and contains two molecules in the unit cell[81] (Figure 20). Several hypotheses were suggested for the character of change in this structure during the transition II—I: the molecular conformation change[77], the rotation of the molecules by the angle 180° around the *W* axis[82], partial disorder of the molecular orientations in phase I[15]. The final conclusion about the conversion mechanism can be drawn only on the basis of the complete data about the structure of the high-temperature phase. However, the presence of the phase transition strongly hinders the growing of high-quality phenanthrene crystals, and, consequently, reliable determination of the structure by diffractional methods has become impossible. At present, it is only known that both phases I and II have the same space group. The unit cell parameters and their temperature dependence have been measured too[80].

In principle, one can solve the problem of the determination of the crystalline structure for organic substances by the atom-atom potential method.

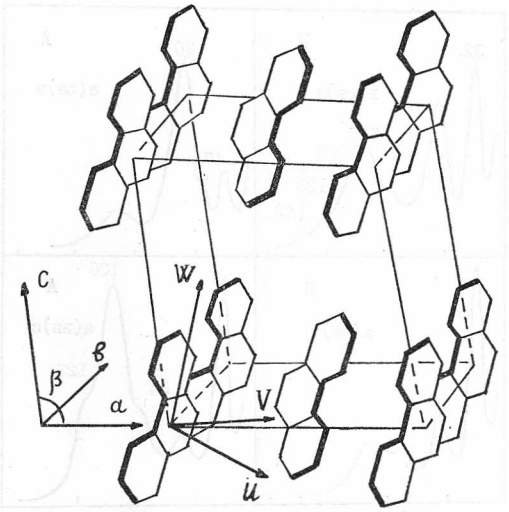

Figure 20. Structure of a phenanthrene crystal at 293 K[81].

Therefore, we have calculated possible molecular packing, low-frequency vibrational spectrum and their changes during the phase transition in phenanthrene. The results of calculations were compared with the temperature dependence measurements of the Raman spectra.

In calculations the atom-atom potentials 6-exp with the Williams parameters were used[52]. The search for the optimal molecular packing in phase I was made by lattice energy minimization at Euler angles for the molecular orientation and coordinates of its mass centre with parameters of the unit cell fixed at 353 K. The calculations for different initial structures resulted in two possible packings (1) and (2) of the molecules in phase I with the lattice energies (kcal/mol):

Temperature	293 K (exp. (83))	293 K	353 K (1)	353 K (2)	
Lattice energy:	22.1 (II)	23.55	22.94 (I)	22.09 (I)	(kcal/mol).

Packing (1) almost coincides with the crystal structure for 293 K and the packing (2) differs from the latter by the molecular rotation around its axes, U, V, W by the Euler angles —4.83°, —31.82°, 24.55°, respectively as well as molecular shifts along the axes a and c^* by —0.09 and 0.18 Å, respectively.

For calculation of the frequencies and normal coordinates of a free phenanthrene molecule the force field obtained in[84] was taken. Relative Raman line intensities were calculated in the oriented gas approximation by the formula (8) using the molecular polarizability tensor measured in[85].

In the low-frequency Raman spectrum of crystalline phenanthrene 9 external (5A + 4B) and 4 internal (2A + 2B) vibrations must be expected which correspond to the low-frequency vibrations of a free molecule: 100 (A_2) and 125 (B_2) cm^{-1} [84] We observed all the expected lines in the monocrystalline Raman spectrum in the polarized radiation at 293 K (Figure 21). In Figure 22 the experimental and the calculated polycrystalline Raman

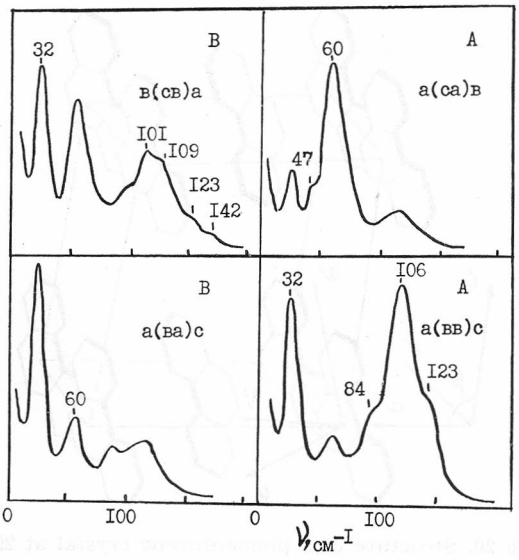

Figure 21. Polarized Raman spectra of the phenanthrene single crystal at 300 K.

spectra at 293 K (phase II) and 353 K (phase I) are presented, and in Table V the appropriate frequency values are given. These data show convincingly that the real structure of phase I is well described by the calculated packing

TABLE V

Experimental and Calculated in the Quasi-Harmonic Approximation Frequencies of Normal Vibrations for Phenanthrene (cm^{-1})

Symm.		Phase II (293 K)		Phase I (353 K)			Interpretation
		Exp.	Calc.	Exp.	Calculation packing (I)	Calculation packing (II)	
	ν_1	142	145.7	—	139.1	178.8	Q (A_2)
	ν_2	125	121.3	—	116.6	163.9	Q (B_2)
	ν_3	106	108.6	96	98.6	127.4	L_w
A	ν_4	84	79.8	—	73.2	102.8	T_u
	ν_5	60	63.7	53	58.8	86.2	L_v
	ν_6	47	49.9	—	46.1	38.9	T_w
	ν_7	(32)	34.0	(27)	30.4	18.8	L_u
	ν_8	142	150.5	—	144.1	175.4	Q (A_2)
	ν_9	109	112.4	—	108.4	152.3	Q (B_2)
	ν_{10}	101	92.5	95	83.3	120.4	L_w
B	ν_{11}	85	76.9	—	70.6	106.4	L_v
	ν_{12}	60	50.1	53	46.0	52.7	T_v, L_v
	ν_{13}	32	22.3	27	21.2	27.9	L_u

Q (A_2) and Q (B_2) are normal coordinates of internal modes 125 cm^{-1} (A_2) and 100 cm^{-1} (B_2) of the free molecule[13], L and T are librations and translational vibrations of molecules with respect to their axes of inertia u, v, w.

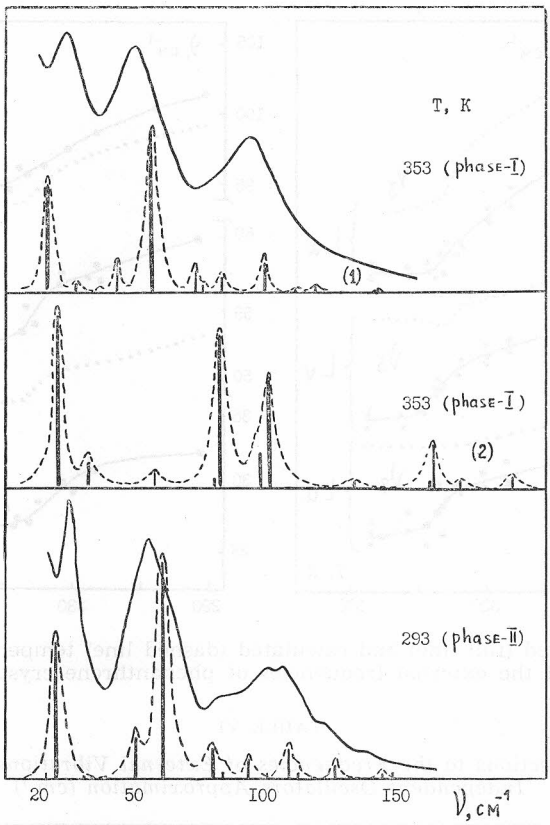

Figure 22. Observed (full line) and calculated (dashed line) Raman spectra of phenanthrene I and phenanthrene II polycrystals.
(1) — calculation with packing 1. (crystal I)
(2) — calculation with packing 2. (crystal I)

(1), which practically coincides with the structure of the phase II (Figure 20). The packing (2) corresponds, possibly, to the structure of the metastable phenanthrene phase observed during the quick cooling of the melt[86].

As it was seen in reference 79, we observed an anomalous temperature dependence of Raman line frequencies in the phase transition region (Figure 23). Both the anomalous thermal expansion of the crystal[80] and the display of the vibrational anharmonicity may be the reasons for that. Using the temperature dependence of unit cell parameters in[80], we have calculated the temperature dependence for external vibration frequencies (packing 1). Anharmonic corrections of the third and the fourth orders were taken into account by means of independent oscillators model by the method proposed in[74]:

$$\nu\,(T) = \nu_{\text{harm}} + \Delta\nu^{(3)} + \Delta\nu^{(4)}$$

where

$$\Delta\nu^{(3)} = -\frac{7.5\,\hbar\,\alpha_3^2}{\nu^4_{\text{harm}}}\,(2n+1), \quad \Delta\nu^{(4)} = \frac{3.0\,\hbar\,\alpha_4}{\nu^2_{\text{harm}}}\,(2n+1)$$

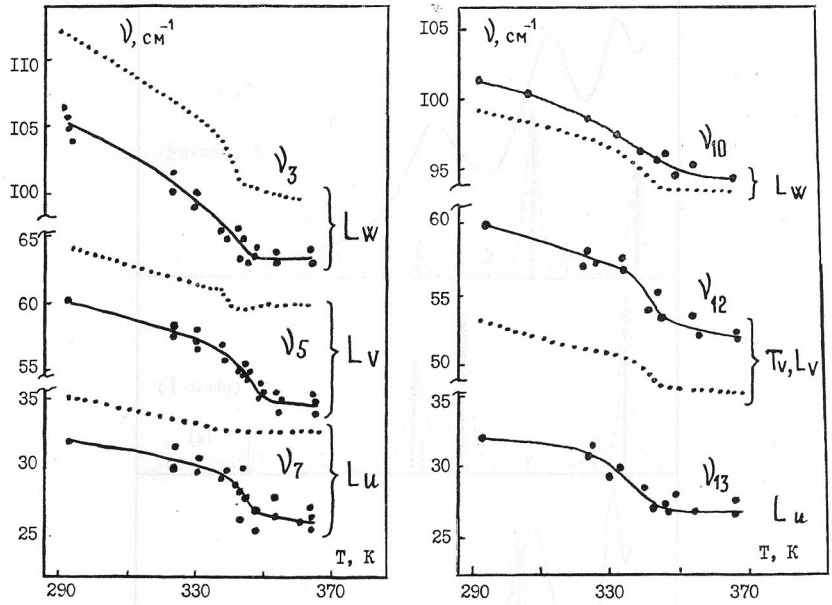

Figure 23. Observed (full line) and calculated (dashed line) temperature dependences of the external frequencies of phenanthrene crystal.

TABLE VI

Anharmonic Corrections to the Frequencies of External Vibrations Calculated in the Independent Oscillators Approximation (cm^{-1})

Symm.		Phase II (293 K)		Phase I, packing (1), (353 K)	
		$\Delta\nu^{(3)}$	$\Delta\nu^{(4)}$	$\Delta\nu^{(3)}$	$\Delta\nu^{(4)}$
A	ν_3	—1.7	3.9	—1.3	2.6
	ν_4	—0.0	2.4	—0.2	3.8
	ν_5	—1.5	3.3	—1.2	5.5
	ν_6	—0.0	1.0	—0.0	2.0
	ν_7	—0.1	0.8	—0.0	2.1
B	ν_{10}	—	5.7	—	9.9
	ν_{11}	—	4.7	—	5.8
	ν_{12}	—	1.2	—	1.9
	ν_{13}	—	23.9	—	32.7

n is phonon number. The anharmonicity constants α_3 and α_4 were derived using the least squares method of the fourth degree polynomial to adjust the »accurate« dependence of the crystal potential energy $U(Q)$ on the normal coordinate calculated by means of atom-atom potentials:

$$1/2\,\nu^2_{\text{harm}}\,Q^2 + \alpha_3\,Q^3 + \alpha_4\,Q^4 \simeq U(Q) - U_o$$

where ν_{harm} is the normal vibration frequency, U_o is the potential energy at the equilibrium position of the molecules. The results of calculation are given

in Table VI and in Figure 23. The calculation presents very well the temperature dependence of the frequencies ν_3 and ν_{10} which correspond to the librational vibrations of molecules around W axis (Figure 20). However, for the other frequencies corresponding to the molecular librations around axes U and V the discrepancies with the experiment are rather large, especially for ν_{13} vibration, where the introduction of anharmonicity corrections increases frequency more than twice (Table VI) indicating that the independent oscillator model does not fit for these vibrations. Thus, in the transition to phase I anharmonic processes of phonon interactions begin to play an important role. One of the probabilities can be a three-phonon process of 60 cm^{-1} (ν_5) phonon decay into two phonons: 30 cm^{-1} (ν_7) and 30 cm^{-1} (ν_{13}).

The investigation of the potential energy minimum shape showed that the two-dimensional cross-section of the energy surface relative to the symmetric rotation of molecules around their axes U and V has the irregular shape of a »ravine« with the bottom becoming practically plane during phase transition II—I (Figure 24). Other cross-sections are of the regular shape

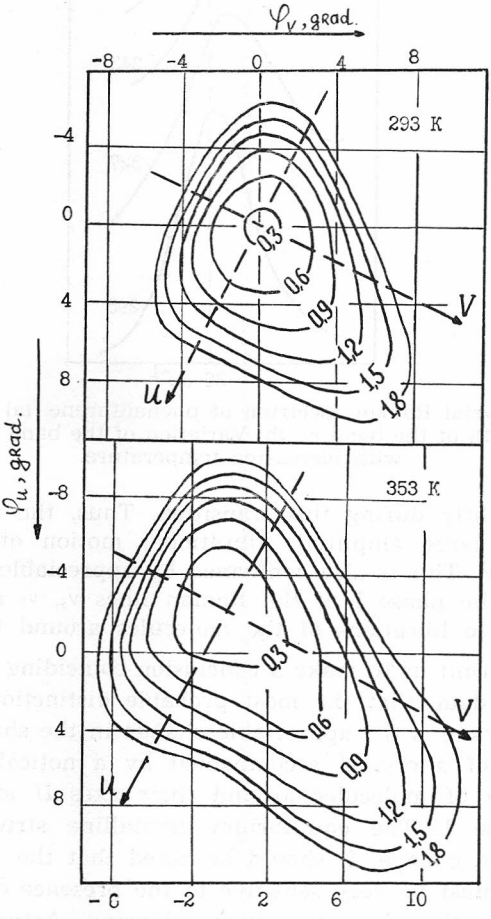

Figure 24. Cross-sections (Kcal/mol) of the potential surface of a phenanthrene crystal as functions of Euler angles Φ_u and Φ_v.

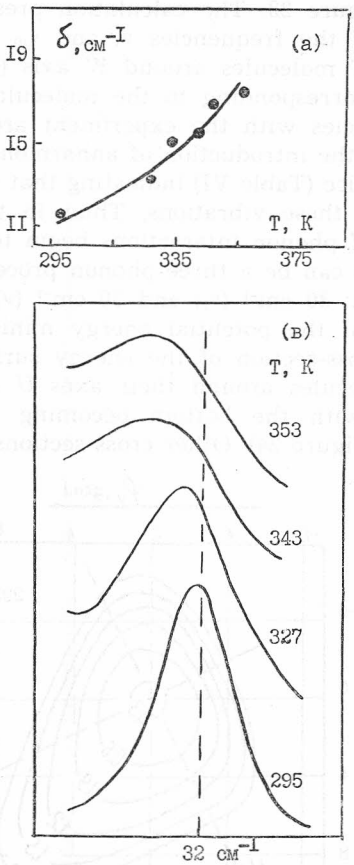

Figure 25. Single crystal Raman spectrum of phenanthrene. (a) Temperature dependence of the linewidth of the band ν_5, (b) Variation of the band shape of the ν_7 mode with increasing temperature.

changing only slightly during this transition. Thus, the calculation predicts the possibility of large amplitude librational motion of molecules around their axes *U* and *V*. This is also confirmed by appreciable broadening during a transition into the phase I of the Raman lines ν_5, ν_7 and ν_{13} (Figure 25), which correspond to librations of the molecules around these axes.

Our studies permit us to make a conclusion coinciding with the calculated and experimental data, that the most probable distinction of a phase transition in phenanthrane is the appreciable change in the shape of the potential energy minimum of a crystal accompanied by a noticable increase in the rotational mobility of molecules around their axes *U* and *V* in the high-temperature phase I. The equilibrium crystalline structure in this case practically does not change. It should be noted that the shape of the lattice energy minimum must be very sensitive to the presence of impurities, which probably results in the phase transition smearing. Actually, as shown in[87], the phase transition in a superpure phenanthrane crystal takes place rather

abruptly at 345 K and is accompanied by mechanical destruction of the specimen, and the introduction of an anthracene admixture smears the transition temperature region.

REFERENCES

1. I. A. Pople and F. E. Karasz, *J. Phys. Chem. Sol.* **18** (1961) 28, *ibid* **20** (1961) 294.
2. L. M. Amzel and L. N. Becka, *J. Phys. Chem. Sol.* **30** (1969) 521.
3. A. R. Ubbelohde, *Melting and Crystal Structure*, Oxford, Clarendon Press, 1965.
4. G. S. Zhdanov, *Kristallografia (USSR)*, **26** (1981) 1301.
5. G. M. Smith, *Plastic Crystals, Liquid Crystals, and the Melting Phenomenon, Adv. in liq. cryst.* **1** (1975) 189.
6. S. N. Vaidya, *Pramana J. Phys.* **12** (1979) 23.
7. V. N. Rogovoi and E. I. Mukhtarov, *Fiz. Tverd. Tela (USSR)* **25** (1983) 1984.
8. N. G. Parsonage and L. A. K. Staveley, *Disorder in Crystals*, Oxford, Clarendon Press, 1978.
9. A. G. Lundin and E. I. Fedin, *NMR-Spectroscopy*, Moscow, Nauka, 1986.
10. W. H. Flygare, *Molecular Structure and Dynamics*, New Jersey, Prentice-Hall, 1978.
11. G. N. Zhizhin, Yu. N. Krasjukov, E. I. Mukhtarov, and V. N. Rogovoi, *Zh. Exp. Teor. Fiz. Pisma (USSR)* **28** (1978) 465.
12. L. A. Leites and S. S. Bukalov, *J. Raman Spectr.* **7** (1978) 235.
13. V. N. Rogovoi, *Phonon Spectra and Phase Transitions in Cyclohexane and Cyclopentane Crystals*, Institute of Spectroscopy, USSR Acad. of Sci., prepr. N 13 (1983).
14. G. Waddington, J. W. Knowlton, and D. W. Scott, *J. Amer. Chem. Soc.* **71** (1949) 797.
15. G. N. Zhizhin, B. N. Mavrin, and V. F. Shabanov, *Opticheskije Kolebatelnyje Spektry Kristallov*, Moscow, Nauka, 1984.
16. V. N. Sidorov, Ju. N. Krasjukov, and E. I. Mukhtarov, *Zh. Prik. Spektros. (USSR)* **43** (1985) 684.
17. G. N. Zhizhin, M. A. Moskaleva, and V. N. Rogovoi, *Zh. Struct. Khim. (USSR)* **14** (1973) 656.
18. D. Andre, P. Fiquier, R. Fourme, M. Ghelfenstein, D. Labarre, and H. Swarc, *J. Phys. Chem. Sol.* **45** (1984) 299.
19. P. R. Fourme, *Acta Cryst.* **B28** (1972) 2984.
20. S. S. Abrahams and W. L. Lipscomb, *Acta Cryst.* **5** (1952) 93.
21. F. Fried, *C. R. Acad. Sci., Paris.* **262** C (1966) 1497.
22. F. Fried and B. Lassier, *J. Chim. phys. et phys. chim. biol.* **63** (1966) 75.
23. R. Fourme, *C. R. Acad. Sci., Paris,* **268** C (1969) 931.
24. L. Colombo and D. Kirin, *Mol. Cryst. Liq. Cryst.* **59** (1980) 85.
25. S. R. Cox, L. Y. Hsu, and D. E. Williams, *Acta Cryst.*, **A37** (1981) 293.
26. G. B. Guthrie, D. W. Scott, W. N. Hubbard, J. P. Catz, M. E. Gross, K. D. Williamson, and G. Waddington, *J. Amer. Chem. Soc.* **74** (1952) 4662.
27. J. P. Marsault and G. Dumas, *C. R. Acad. Sci., Paris.* **264 B** (1967) 782.
28. C. J. Jakobs, *J. Amer. Chem. Soc.* **56** (1934) 1513.
29. A. I. Kitaigorodskii, *Molecular Crystals, Moscow*, Nauka, 1971.
30. A. I. Kitaigorodskii and E. I. Mukhtarov, *Fiz. Tverd. Tela (USSR)* **10** (1968) 3474.
31. G. S. Pawley, *Phys. Status Solidi* **20** (1967) 347.
32. E. I. Mukhtarov, V. N. Rogovoi, Ju. N. Krasjukov, and G. N. Zhizhin, *Optika i spektros. (USSR)* **46** (1979) 920.
33. N. V. Sidorov, Ju. N. Krasjukov, E. I. Mukhtarov, and G. N. Zhizhin, *Khim. Fizika (USSR)* **10** (1982) 1320.
34. G. Fillipini, O. M. Gramaccioli, and M. Simonetta, *J. Chem. Phys.* **59** (1973) 5088.
35. W. D. Ellensen and M. Nuol, *J. Chem. Phys.* **61** (1974) 1380.

36. G. Taddei, H. Bonadeo, M. P. Marzocci, and S. Califano, *J. Chem. Phys.* **58** (1973) 966.
37. E. Burgos, H. Bonadeo, and E. D'Alessio, *J. Chem. Phys.* **63** (1975) 38.
38. P. J. Bounds and R. W. Munn, *J. Chem. Phys.* **24** (1977) 343.
39. G. S. Pawley, A. M. Brass, and M. T. Dove, *J. Chim. Phys.* **82** (1985) 249.
40. T. B. Reed and W. N. Lipscomb, *Acta Cryst.* **6** (1953) 45.
41. K. S. Pitzer, *J. Amer. Chem. Soc.* **62** (1940) 331.
42. H. S. Gutowaky and G. E. Pake, *J. Chem. Phys.* **18** (1950) 162.
43. A. Ozora, T. Nakagawa, and M. Ito, *Bull. Chem. Soc. Japan.* **45** (1972) 95.
44. J. R. Durig, K. K. Lau, and S. E. Hannum, *J. Mol. Struct.* **9** (1971) 291.
45. J. D. Hoffman and B. F. Decker, *J. Phys. Chem.* **57** (1953) 520.
46. M. Suzuki, T. Yokoyama, and M. Ito, *Spectrochim. Acta* **24A** (1968) 1091.
47. I. Harada and T. Shimanouchi, *J. Chem. Phys.* **44** (1966) 2016.
48. A. V. Korshunov and A. V. Sechkarev, in: *Sovremennyje problemy spektroskopii kombinazionnogo rassejanija sveta,* Moskwa, Nauka, 1978, p. 170.
49. P. A. Bazhulin and A. A. Rakhimov, *Fiz. Tverd. Tela (USSR)* **8** (1966) 2167.
50. J. C. Bellows and P. N. Prasad, *J. Chem. Phys.* **70** (1979) 1864.
51. A. I. Kitaigorodskii and E. I. Mukhtarov, *Opt. i Spektros. (USSR)* **32** (1971) 706.
52. D. E. Williams, *J. Chem. Phys.* **45** (1966) 3770.
53. D. W. Crushank, *Acta Cryst.* **10** (1957) 507.
54. E. I. Mukhtarov and A. A. Pichurin, *Opt. i Spektros. (USSR)* **34** (1973) 1143.
55. G. Ya. Kirsanov, A. A. Artamonov, and A. V. Sechkarev in: *Spektroskopiya i jeje Primenenije v Geofizike i Khimii,* Novosibirsk, Nauka, 1975, p. 281.
56. P. M. Robinson, H. J. Kossel, H. G. Scott, and C. Legge, *Mol. Cryst. Liq. Crysta.* **11** (1970) 105.
57. V. V. Kind, *Dissertation,* Krasnojarsk, 1980.
58. R. M. Nacfarlane and S. Ushioda, *J. Chem. Phys.* **67** (1977) 3214.
59. S. McGuigan, J. H. Strange, and J. M. Chezean, *Mol. Phys.* **49** (1983) 175.
60. J. G. Aston, G. J. Szasz, and H. L. Fink, *J. Amer. Chem. Soc.* **65** (1943) 1135.
61. R. Kahn, R. Fourme, and D. André, *Acta Cryst.* **B29** (1973) 131.
62. G. E. Bacon, N. A. Curry, and S. A. Wilson, *Proc. Roy. Soc.* **279A** (1964) 98.
63. E. G. Cox, D. W. Cruicshank, and I. A. Smith, *Proc. Roy. Soc.* **277 A** (1958) 1.
64. E. R. Andrew and R. G. Eades, *Proc. Roy. Soc.* **216A** (1953) 398.
65. S. B. W. Roeder and D. C. Douglass, *J. Chem. Phys.* 52 (1970) 5525.
66. E. R. Andrew and R. G. Eades, *Proc. Roy. Soc.* **218A** (1953) 537.
67. J. E. Anderson, *J. Chem. Phys.* **43** (1965) 3475.
68. D. A. Wright, R. K. Boyd, and C. A. Fyfe, *J. Phys. Chem. Sol.* 35 (1974) 1355.
69. A. Gavezzotti and M. Simoneta, *Acta Cryst.* **A32** (1976) 997.
70. H. Bonadeo, M. P. Marzocchi, E. Castelluci, and S. Califano, *J. Chem. Phys.* **57** (1972) 4299.
71. V. N. Rogovoi and G. N. Zhizhin, *Fiz. Tverd. Tela (USSR)* **17** (1975) 376.
72. B. P. Nevsorov and A. V. Sechkarev, *Izv. Vuzov (ser. fiz.) (USSR)* **2** (1971) 75.
73. Y. A. Sotaty and A. Ron, *Chem. Phys. Lett.* **25** (1974) 384.
74. B. Kuchta and T. Luty, *J. Chem. Phys.* **78** (1983) 1447.
75. G. Dumas, M. P. Chedin, and F. Vovelle, *J. de Phys.* **41** (1980) 905.
76. S. Matsumoto and T. Tsukada, *Bull. Chem. Soc. Jap.* **38** (1965) 2023.
77. D. H. Spielberg, R. A. Arndt, A. C. Damask, and L. Lefkowits, *J. Chem. Phys.* **54** (1971) 2597.

78. S. Matsumoto, *Bull. Chem. Soc. Jap.* **39** (1966) 1811.
79. L. Colombo, *Chem. Phys. Lett.* **48** (1973) 166.
80. S. Matsumoto and T. Fukuda, *Bull. Chem. Soc. Jap.* **40** (1967) 747.
81. J. Kay, Y. Okaya, and D. E. Cox, *Acta Cryst.* **B27** (1971) 26.
82. G. Baranovic and V. Volovsek, *J. Mol. Struct.* **143** (1986) 29.
83. C. G. DeKraiff, *J. Chem. Thermodyn.* **12** (1980) 243.
84. G. Fillippini, M. Simonetta, and C. M. Gramaccioli, *Mol. Phys.* **51** (1984) 445.
85. P. J. Bounds and R. W. Munn, *Chem. Phys.* **24** (1977) 343.
86. G. N. Zhizhin, Yu. N. Krasjukov, E. I. Mukhtarov, and N. V. Sidorov, *Raman Low Frequency Spectroscopic Study of the Phase Transition in the Phenantrene Crystal,* Institute of Spectroscopy, USSR Acad. of Sci., prepr. N 6 (1987).
87. B. J. McArdle, J. N. Sherwood, and A. C. Damask, *J. Cryst. Growth* **22** (1974) 193.

SAŽETAK

Proučavanje reorjentacijskih kretanja molekula u kristalima pomoću Ramanove spektroskopije niskih frekvencija

G. N. Zhizhin, Yu. N. Krasjukov, E. I. Mukhtarov, V. N. Rogovoi i N. V. Sidorov

Opisana su istraživanja reorjentacijskih pojava u organskim kristalima pomoću temperaturne ovisnosti vibracijskih spektra niske frekvencije i istovremenog računanja molekularne dinamike po AAP metodi.